Proc. Natl. Acad. Sci. USA
Vol. 96, pp. 9926–9931, August 1999
Neurobiology

Cytoplasmic amino and carboxyl domains form a wide intracellular vestibule in an inwardly rectifying potassium channel

TAO LU, YONG-GANG ZHU, AND JIAN YANG*

Department of Biological Sciences, Columbia University, New York, NY 10027

Edited by Lily Yeh Jan, University of California, San Francisco, CA, and approved June 18, 1999 (received for review April 2, 1999)

ABSTRACT **We have studied the structural components and architecture of the intracellular vestibule of a strongly rectifying channel (Kir2.1) expressed in *Xenopus* oocytes. Putative vestibule-lining residues were identified by systematically examining covalent modification by sulfhydryl-specific reagents of cysteine residues engineered into two cytoplasmic regions. In a stretch of 33 amino acids in the amino terminus (from C54 to V86) and 22 amino acids in the carboxyl terminus (from R213 to S234), 15 and 11 residues, respectively, were found to be accessible to methanethiosulfonate ethylammonium (MTSEA) or methanethiosulfonate ethyltrimethylammonium (MTSET) and presumably project into the aqueous intracellular vestibule. The pattern of accessibility suggests that both stretches may adopt an extended loop structure. To explore the physical dimension of the intracellular vestibule, we covalently linked a constrained number (one to four) of positively charged moieties of different sizes to the E224 position and found that this vestibule region is sufficiently wide to accommodate four modifying groups with dimensions of 12 Å × 10 Å × 6 Å. These results suggest that regions in both the amino and carboxyl domains of Kir2.1 channel form a long and wide intracellular vestibule that protrudes beyond the membrane into the cytoplasm.**

Inwardly rectifying K^+ (Kir) channels play an important role in controlling the resting membrane potential and cell excitability (1). They conduct more efficiently when the membrane potential is negative than when it is positive to the K^+ equilibrium potential (2). This inward rectification arises from voltage- and external K^+-dependent block of the internal pore by intracellular Mg^{2+} (3–10) and polyamines (11–13). The internal pore consists of an inner pore formed by membrane-spanning segments and an intracellular vestibule that protrudes from the membrane into the cytoplasm. The vestibule region forms a low-resistance access pathway to the inner pore and may contain residues that are important for Mg^{2+} and polyamine block. Delineation of the molecular architecture of this region is thus valuable for understanding the mechanism of inward rectification as well as ion permeation.

Kir channel subunits have a relatively short cytoplasmic amino terminus, followed by two membrane-spanning segments (M1 and M2) with a K^+ selectivity filter-forming P loop in between, and a long cytoplasmic carboxyl terminus (14, 15). This transmembrane topology resembles that of a K^+ channel, KcsA, from *Streptomyces lividans*. The three-dimensional crystal structure of the KcsA channel shows that four M2 segments form an inner pore consisting of a 10-Å-wide cavity in the center of the membrane bilayer and a 6-Å-wide tunnel opening to the cytoplasm (16). Using the substituted-cysteine accessibility method (SCAM) (17, 18), we have recently shown that the inner pore of a strong inward rectifier channel, Kir2.1, is also formed by the M2 segment but is significantly wider, with a diameter of >12 Å (19). Furthermore, there is evidence that both the cytoplasmic amino and carboxyl termini of Kir channel subunits contribute to form an intracellular vestibule leading toward the inner pore formed by the M2 segment (10, 20–22). For example, a negatively charged residue in the carboxyl terminus, E224, was found to be critical for ion permeation and high-affinity Mg^{2+} and polyamine binding (20, 21). However, there is yet no detailed information about which regions of the cytoplasmic domains and which residues participate in forming the intracellular vestibule.

In this study, we investigated the structural components and architecture of the intracellular vestibule of Kir2.1 channels expressed in *Xenopus* oocytes. The method and experimental procedures closely paralleled those of our previous work on the M1 and M2 transmembrane segments (19). We first used SCAM to identify putative vestibule-lining residues. Thirty-three and 22 consecutive residues in an amino-terminal segment immediately adjacent to M1 and a carboxyl-terminal segment encompassing E224, respectively, were individually mutated to cysteine. The side-chain accessibility of the engineered cysteines was determined by means of irreversible current alteration by methanethiosulfonate ethylammonium (MTSEA) and/or methanethiosulfonate ethyltrimethylammonium (MTSET) applied to the intracellular side of the mutant channels in giant inside-out patches. We next examined the physical dimensions of the intracellular vestibule at the E224 locus by exploiting a concatenation approach to control the stoichiometry of modification such that we were able to link various numbers (from one to four) of modifying reagents of different sizes to the intracellular vestibule. Our results suggest a long and wide intracellular vestibule formed by cytoplasmic regions from both the amino and carboxyl domains.

MATERIALS AND METHODS

Site-directed mutagenesis, construction of tandem tetramers, oocyte expression, patch-clamp recordings, and data analysis were performed as described previously (19). The bath solution contained 110 mM KCl, 10 mM Hepes, 9 mM EGTA, 1 mM EDTA, 200 μM $CaCl_2$, 5 mM KF, and 0.1 mM $NaVO_3$ (pH 7.3 with KOH). The pipette solution contained 130 mM KCl, 10 mM Hepes, and 3 mM $MgCl_2$ (pH 7.3 with KOH).

Methanethiosulfonate (MTS) reagents (Toronto Research Chemicals, North York, ON, Canada) and monobromotrimethylammoniobimane bromide (qBBr; Molecular Probes) were stored at −20°C and were dissolved in bath solution prior to each experiment, generally <1 min before application. MTSEA (2.5 mM), MTSET (2 mM), or qBBr (4 mM) was

The publication costs of this article were defrayed in part by page charge payment. This article must therefore be hereby marked "*advertisement*" in accordance with 18 U.S.C. §1734 solely to indicate this fact.

PNAS is available online at www.pnas.org.

This paper was submitted directly (Track II) to the *Proceedings* office.
Abbreviations: SCAM, substituted-cysteine accessibility method; MTS, methanethiosulfonate; MTSEA, methanethiosulfonate ethylammonium; MTSET, methanethiosulfonate ethyltrimethylammonium; qBBr, monobromotrimethylammoniobimane bromide; Kir channels, inwardly rectifying K^+ channels.
*To whom reprint requests should be addressed at: Department of Biological Sciences, 915 Fairchild Center, MC2462, Columbia University, New York, NY 10027. E-mail: jy160@columbia.edu.

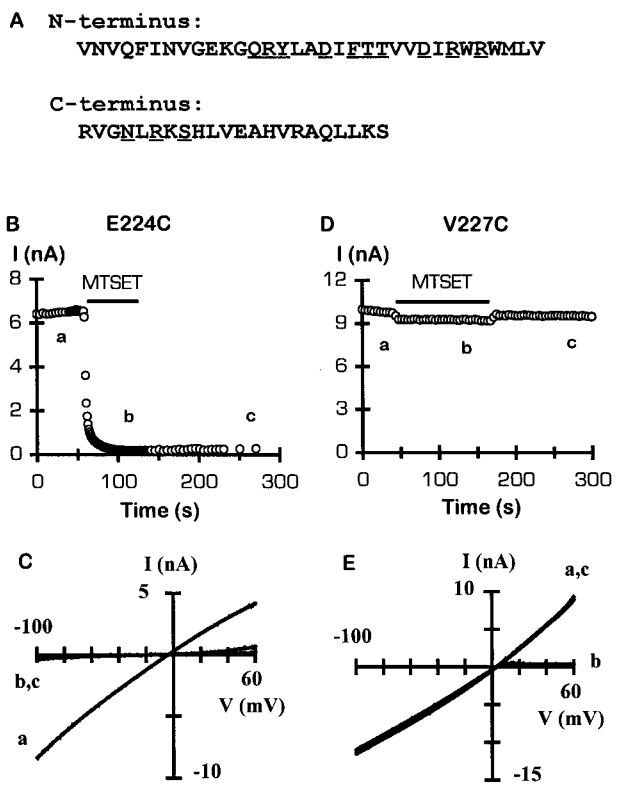

FIG. 1. (*A*) Amino acids in the amino- and carboxyl-terminal domains of IRK1J subunit that were individually mutated to cysteine. The amino- and carboxyl-terminal sequence is from residues 54–86 and 213–234, respectively. Mutation of the underlined residues to cysteine resulted in nonfunctional homomeric channels. (*B–E*) Effect of internal MTSET on E224C or V227C channels. (*B* and *D*) Time course of inhibition of inward current (sign reversed) at −80 mV by 2 mM MTSET, applied for 1 (*B*) or 2 (*D*) min to the intracellular side of a giant inside-out patch. Current sampling interval was changed to 1 s during MTSET application in *B*. (*C* and *E*) Current–voltage (I–V) relations from the corresponding patch, before (trace a), during (trace b), and after (trace c) MTSET application. Current was generated by voltage ramps from −100 mV to +80 mV over 70 ms. Notice that the I–V relation for V227C channels obtained in the presence of MTSET exhibits strong inward rectification (trace b), which is reversible after washout of MTSET (trace c).

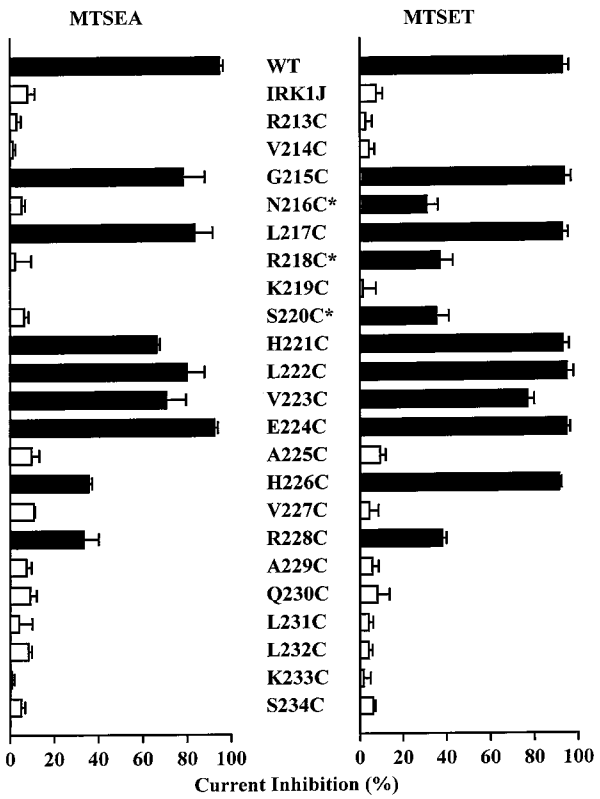

FIG. 2. Effect of internal MTSEA and MTSET on carboxyl-terminal cysteine mutant channels. Bars represent steady-state inhibition of current at −80 mV by 2.5 mM MTSEA or 2 mM MTSET applied to the intracellular side. The responses of the wild-type and IRK1J channels are shown for comparison. Current was elicited by voltage ramps from −100 mV to +80 mV over 70 ms from a holding potential of −40 mV. Black bars indicate responses that are significantly different from the response of IRK1J channels ($P < 0.05$). Error bars represent SD (n = 3–6). Mutant channels rescued by tandem tetramers are marked with an asterisk.

applied for 2–8 min until modification reached steady state. For V61C and E224C mutant channels, 20 μM MTSET was used in experiments to determine its reaction rate. The effect of a reagent was calculated from the current amplitude measured at −80 mV, obtained before application and after washout of the reagent. No corrections were made for leakage current or for current run-down, which was generally negligible. The time constant of modification was obtained by fitting the time course with a single exponential. The apparent second-order rate constant of MTSEA and MTSET reaction with the cysteine mutant channels was then calculated as the reciprocal of the time constant divided by the concentration. Data are presented as mean ± SD (number of observations). Statistical testing was with Student's t test.

RESULTS

Rescuing Nonfunctional Cysteine Mutants by Using Tandem Tetramers. In our previous study on the architecture of the inner pore of Kir2.1 channels, we found that the wild-type Kir2.1 channel was inhibited by both internal and external MTS reagents and, therefore, we mutated six endogenous cysteine residues and created a nonreactive channel named IRK1J (19). In this study, we used IRK1J as the control channel and constructed all cysteine mutations on this background. We replaced, one by one, 33 consecutive residues (V54–V86) in the amino terminus (immediately adjacent to the first membrane-spanning segment, M1) and 22 consecutive residues (R213–S234) in the carboxyl terminus of IRK1J subunit with a reporter cysteine residue (Fig. 1*A*). Most mutant subunits formed functional homotetrameric channels when expressed in *Xenopus* oocytes. However, 13 mutants failed to generate measurable whole-cell current (underlined residues in Fig. 1*A*). To rescue their function, we employed a strategy of concatenating four subunits into a tandem tetramer (23). It has been shown that four Kir2.1 subunits linked head-to-tail in a single protein chain can preferentially coassemble to form functional channels identical to the channel formed by four individual subunits (19, 24), and that such an approach can be used to salvage function from "lethal" mutations that result in nonfunctional channels (25). We applied this rescuing strategy to the 13 "lethal" cysteine mutants by linking three IRK1J subunits with one mutant subunit, creating a tandem tetramer of IRK1J-IRK1J-IRK1J-X, where X stands for the cysteine mutant subunit. All 13 tandem tetramers constructed in this fashion produced functional channels in oocytes. A caveat is that these channels contain only one reporter cysteine residue instead of four as in channels formed by four monomeric mutant subunits.

All mutant channels, formed by either monomers or tandem tetramers, retained high selectivity for K^+ over Na^+ and showed strong inward rectification, except E224C, which exhibited a weaker rectification (data not shown).

Accessible Residues in the Carboxyl Domain. We first tested the accessibility of E224C because this glutamate residue has been shown to be critical for ion permeation as well as Mg^{2+} and polyamine blocking (20, 21) and, therefore, is expected to project into the aqueous vestibule. Indeed, application of 2 mM MTSET to the cytoplasmic side of E224C channels rapidly and irreversibly abolished the current (Fig. 1 *B* and *C*). By contrast, channels containing a mutation of an adjacent residue, V227C, were not irreversibly inhibited by MTSET (Fig. 1 *D* and *E*). In this case, however, the outward current was reversibly inhibited, resulting in an inward rectification as seen with IRK1J channels (19).

Fig. 2 summarizes the steady-state effect of internal application of 2.5 mM MTSEA or 2 mM MTSET on the carboxyl-terminal cysteine mutant channels. Eleven of the 22 mutant channels showed various degrees of inhibition by MTSET. The magnitude of steady-state inhibition was 31% to 95%. For some mutant channels, a 2-min application was sufficient to accomplish steady-state inhibition, whereas for others, a 5-min application was required to achieve the full effect (Table 1). Table 1 shows the apparent second-order rate constant of MTSET modification, obtained by fitting the time course of current inhibition with a single exponential function. With the exception of E224C, the reaction rate constant for all mutant channels is much slower than the reported $\approx$90,000 $M^{-1}\cdot s^{-1}$ reaction rate of MTSET with 2-mercaptoethanol (26).

One mutant channel, K219C, showed an augmentation of 42 ± 22% (n = 5) after covalent modification by MTSEA. In contrast, MTSET did not have a significant effect (Fig. 2). Interestingly, in patches pretreated with MTSET, subsequent application of MTSEA failed to increase the current (data not shown), indicating that the reporter cysteine residues had already been covalently modified by MTSET and that such modification was functionally silent.

Accessible Residues in the Amino Domain. The steady-state effects of internal application of 2.5 mM MTSEA or 2 mM MTSET on 33 amino-terminal cysteine mutant channels are summarized in Fig. 3. Altogether, 15 mutant channels were inhibited by MTSET. One mutant channel, K64C, behaved similarly to K219C. Its current was increased by 79 ± 30% (n = 5) after covalent modification by MTSEA but was unaffected after covalent modification by MTSET. In channels inhibited by MTSET, the magnitude of steady-state inhibition varied from 21% to 99% (Table 1). Among mutant channels formed by monomeric subunits, five showed >90% current inhibition (V54C, F58C, V61C, I79C, and W81C) and three showed only partial (34–60%) inhibition (L69C, V76C, and W83C). The two cysteines present in the wild-type subunit, C54 and C76, are clearly modifiable and thus contribute to the reactivity of the wild-type channel. All reactive channels formed by tandem tetramers were only partially (21–46%) inhibited. As is the case for the carboxyl terminus, the apparent second-order rate constant of MTSET modification (Table 1) is much lower than that of MTSET reaction with free 2-mercaptoethanol.

An unexpected result is that the M84C mutant channel was not affected by internal MTSEA or MTSET. This result appears to contradict that of a previous study, which showed that a lysine residue at the analogous position in Kir1.1 channels could be titrated by intracellular protons, and that when M84 in Kir2.1 channels was mutated to lysine, they also became sensitive to intracellular pH (22). We do not yet fully understand this discrepancy. It is possible that M84 is exposed to the water-accessible surface, but its orientation and/or environment hampers access of MTSEA and MTSET but not protons.

Differential Effects of MTSEA and MTSET. The reactive cysteines identified above are likely on the water-accessible surface of the channel and can face either the lumen of the intracellular vestibule or the cytoplasm. Covalent modification of these cysteines can result in channel inhibition either directly through blockade of the vestibule or indirectly through an allosteric mechanism. Comparisons of modification by MTSEA and MTSET suggest that the reactive cysteines probably line the surface of the vestibule. There are two significant differences in the effects of MTSEA and MTSET. First, a number of mutant channels formed by monomers (F58C and W83C) as well as tandem tetramers (Q66C, R67C, Y68C, D71C, D78C, N216C, R218C, and S220C) were not significantly affected by MTSEA but were clearly inhibited by MTSET (Figs. 2 and 3). The F58C mutant channel was a particularly striking example (Fig. 4 *A* and *B*). Whereas 2 mM internal MTSET completely and irreversibly diminished the

Table 1. Inhibition of current by internal MTSET

Amino-terminal mutants				Carboxyl-terminal mutants			
	% inhibition				% inhibition		
Channel	2 min	5 min	k, $M^{-1}\cdot s^{-1}$	Channel	2 min	5 min	k, $M^{-1}\cdot s^{-1}$
WT	93 ± 3		19 ± 1	WT	93 ± 3		19 ± 1
V54C	44 ± 12	91 ± 3	4.3 ± 1.9	G215C	74 ± 8.6	94 ± 3	6.6 ± 1.4
F58C	77 ± 4	94 ± 2	6.3 ± 1.2	N216C*	31 ± 5	ND	16 ± 8
V61C	99 ± 0.6	ND	2,600 ± 608	L217C	93 ± 3	ND	9.3 ± 1.5
Q66C*	21 ± 2	ND	5 ± 2	R218C*	26 ± 1	37 ± 6	6.6 ± 2.2
R67C*	16 ± 6	26 ± 5	3.8 ± 1.4	S220C*	35 ± 6	ND	28 ± 2
Y68C*	21 ± 3	28 ± 4	4.5 ± 0.6	H221C	77 ± 11	93 ± 3	6.8 ± 2.0
L69C	38 ± 5	60 ± 5	3.2 ± 0.3	L222C	76 ± 10	95 ± 3	8.3 ± 1.5
D71C*	20 ± 4	ND	22 ± 12	V223C	43 ± 5	77 ± 3	2.4 ± 1.0
T74C*	29 ± 5	41 ± 7	3.3 ± 0.3	E224C	95 ± 2	ND	2,217 ± 189
T75C*	41 ± 1	46 ± 3	6.5 ± 1.3	H226C	91 ± 1	ND	25 ± 1
V76C	19 ± 4	34 ± 9	2.0 ± 0.7	R228C	38 ± 2	ND	35 ± 3
D78C*	46 ± 3	ND	17 ± 6				
I79C	92 ± 1	ND	58 ± 19				
W81C	64 ± 7	92 ± 1.3	7.3 ± 4.5				
W83C	32 ± 3	56 ± 3	2.9 ± 0.5				

MTSET was applied at 2 mM to the intracellular side of giant inside-out patches containing the wild-type or mutant channels for 2 or 5 min, depending on the reaction rate to reach the steady-state effect. For V61C and E224C, 20 μM MTSET was used in experiments to determine the reaction rate (the right-hand column). Only reactive channels are shown. Percentage inhibition and the apparent second-order rate constant k were calculated as described in *Materials and Methods*. ND, not determined, because steady-state inhibition was achieved in 2 min. Data are presented as mean ± SD (n = 3–6).
*Mutants rescued by tandum tetramers.

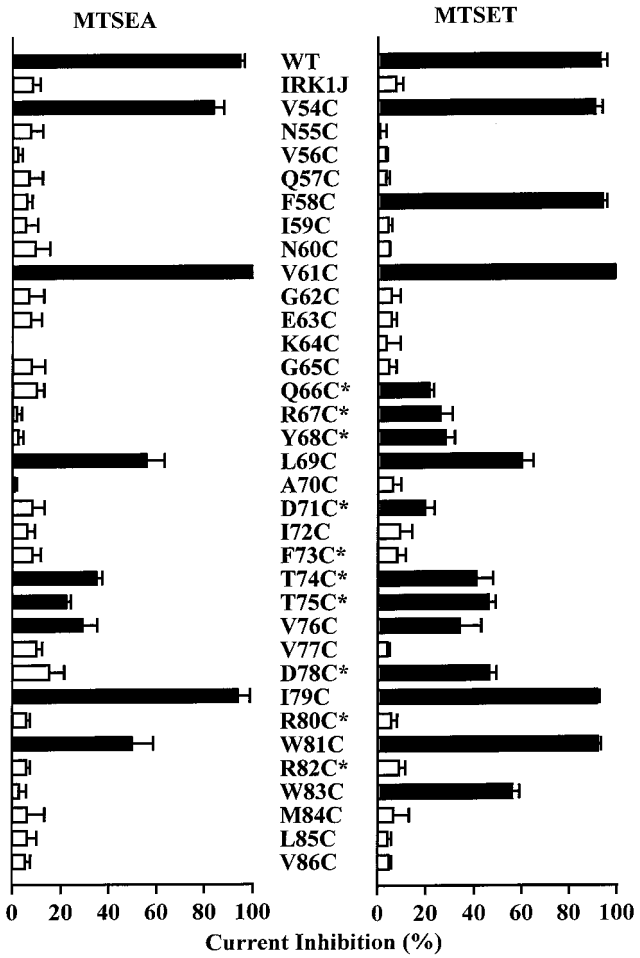

FIG. 3. Effect of internal MTSEA and MTSET on amino-terminal cysteine mutant channels. Bars represent steady-state inhibition of current at −80 mV by 2.5 mM MTSEA or 2 mM MTSET applied to the intracellular side. The responses of wild-type and IRK1J channels are shown for comparison. Current was elicited by voltage ramps from −100 mV to +80 mV over 70 ms from a holding potential of −40 mV. Black bars indicate responses that are significantly different from the response of IRK1J channels ($P < 0.05$). Error bars represent SD (n = 3–6). Mutant channels rescued by tandem tetramers are marked with an asterisk.

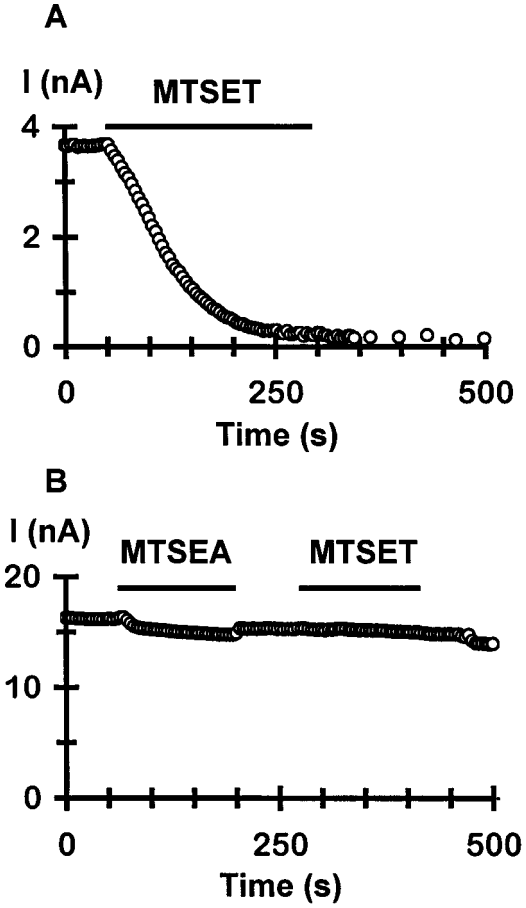

FIG. 4. Differential effect of MTESA and MTSET. (*A*) Time course of irreversible inhibition of F58C channels by 2 mM internal MTSET. (*B*) Effect of internal MTSEA and then MTSET on F58C channels from another patch. Notice that after a 2-min application of 2.5 mM MTSEA, subsequent application of 2 mM MTSET no longer produced irreversible inhibition of the current. In both cases, current was elicited by voltage ramps from −100 mV to +80 mV over 70 ms from a holding potential of −40 mV at a 4-s interval, and the current amplitude at −80 mV was plotted.

current (Fig. 4*A*), 2.5 mM MTSEA had little irreversible effect (Fig. 4*B*). Interestingly, after washout of MTSEA, subsequent application of MTSET to the same patch no longer produced irreversible reduction of the current (Fig. 4*B*). This observation indicates that MTSEA did form a covalent linkage with the engineered cysteines and, hence, prevented them from subsequent reaction with MTSET, but such a covalent modification by MTSEA did not affect channel activity. The same results were also obtained for all the residues indicated above. Second, with the exception of K64C and K219C, MTSET produced the same or more steady-state inhibition than MTSEA in all reactive mutant channels (Figs. 2 and 3). These results, taken together, are consistent with a simple pore-blocking effect caused by the covalently attached modifying moieties.

A Wide Intracellular Vestibule Revealed by Stoichiometric Covalent Modification. We next sought to explore the physical dimensions of the intracellular vestibule by using a method described previously (19). The strategy was to gauge the vestibule with sulfhydryl-specific reagents of various sizes covalently linked to a key position in the vestibule. Because of its functional importance we chose position E224. Using tandem tetramers that contained a constrained number (from one to four) of E224C subunits, we were able to obtain singly, doubly, triply, and quadruply modified channels. The modifying reagents used include MTSEA, MTSET (head-group diameter, 3.6 Å and 5.8 Å, respectively), and qBBr, which is more rigid and larger, with dimensions of 12 Å × 10 Å × 6 Å (19, 27). Fig. 5 summarizes the steady-state effect of these reagents on channels containing from zero to four E224C subunits. Clearly, for each reagent, the channels with one, two, or three modifiable cysteines were not completely blocked and there is a striking correlation between the magnitude of the block and the number of modifiable subunits in the channel. As expected, the much larger qBBr produced a more severe effect than did MTSEA and MTSET in the partially modified channels. We interpret these results to suggest that for each reagent, all four subunits making up the channel must to be modified to completely block ion conduction. These results suggest that the vestibule harboring residue E224 may be wide enough to simultaneously accommodate four groups with dimensions of 12 Å × 10 Å × 6 Å.

DISCUSSION

Structure–function studies on K^+ channel permeation have been primarily focused on pore regions formed by the P loop and transmembrane segments. By contrast, the cytoplasmic vestibule region leading toward the pore has not been char-

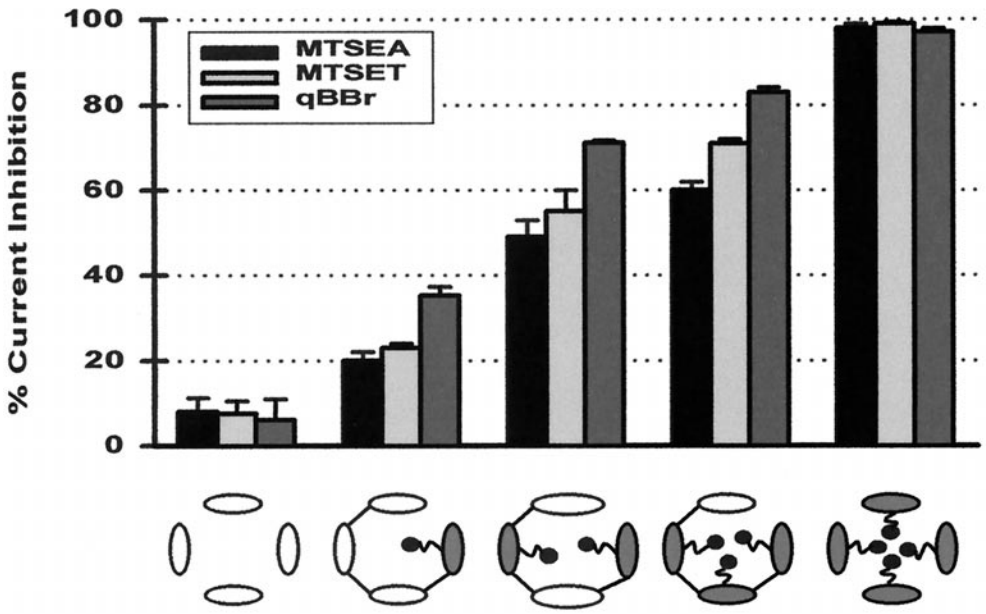

FIG. 5. Sizing the intracellular vestibule by using stoichiometric covalent modification. The bar graph illustrates the steady-state inhibition of current at −80 mV by MTSEA, MTSET, and qBBr in channels containing zero to four E224C subunits. The channel type is depicted by the schematic underneath the bar graph, with open ovals representing the control IRK1J subunit and filled ovals representing the E224C subunit. Current was elicited in giant inside-out patches by voltage ramps from −100 mV to +80 mV over 70 ms from a holding potential of −40 mV. Percentage inhibition was calculated from the current at −80 mV before application and after washout of a modifying reagent. Steady-state inhibition in the five types of channels was 8.0 ± 3.2%, 20 ± 2%, 44 ± 1%, 60 ± 2%, and 98% by 2.5 mM MTSEA, 7.5 ± 3%, 23 ± 1%, 55 ± 5%, 71 ± 1%, and 99% by 2 mM MTSET, and 6 ± 5%, 35.3 ± 2.1%, 71.7 ± 0.6%, 83 ± 1.1%, and 97 ± 1.0% by 4 mM qBBr. For MTSET and qBBr, steady-state modification was confirmed by the lack of further inhibition upon subsequent application of 2.5 mM MTSEA.

acterized in detail despite its functional importance. In this study, we have used SCAM to identify a large number of amino acids in the cytoplasmic amino- and carboxyl-terminal domains that presumably line the lumen of the intracellular vestibule of Kir2.1 channels. Furthermore, the results of stoichiometric covalent modification with reagents of various sizes led us to conclude that the intracellular vestibule is very wide, probably with a diameter of >20 Å.

SCAM has been widely used to identify pore-lining residues in membrane-spanning segments of various types of ion channels (18). A key assumption in interpreting SCAM results is that positions accessible to charged, water-soluble thiol-specific reagents line the aqueous ion-conducting pathway. This assumption has been tested repeatedly in transmembrane regions and seems reasonable for them (18). However, interpretation of SCAM results for a cytoplasmic region is complicated by the fact that an exposed cysteine can face either the vestibule or the cytoplasm. It is possible that a cysteine located outside the vestibule can react with a MTS reagent, and the resultant covalent modification can inhibit channel activity through an allosteric mechanism. The differential effect of MTSEA and MTSET is suggestive but not definitive that most reactive cysteines face the vestibule. As shown in Figs. 2 and 3, all the reactive mutant channels were inhibited by MTSET to the same or a larger degree than by MTSEA. Although we cannot rule out an allosteric effect, it seems unlikely that a set of conditions exists for all the reactive residues such that MTSET always produces a greater effect on ion conduction than does MTSEA through a purely allosteric mechanism. An alternative interpretation, which we feel is more straightforward and logical, is that the reactive cysteine residues line the surface of the intracellular vestibule such that covalent linkage of the larger -S-CH_2-CH_2-N$(CH_3)_3^+$ moiety from MTSET always exerts a more profound steric and electrostatic hindrance to ion conduction than the smaller -S-CH_2-CH_2-NH_3^+ group from MTSEA.

The reaction rate of MTSET with most of the reactive cysteine mutant channels (Table 1) was much (1,600- to 45,000-fold) slower than that of MTSET with free thiols in solution (26). However, these reaction rates are comparable to the rate of MTSET modification of pore-lining residues in the M2 of Kir2.1 channels (19), including G168, C169, D172, A173, and I176, whose analogous positions in KcsA channels have been directly demonstrated to project to the pore by x-ray crystallography (16). As we discussed in detail in our previous study (19), the paradoxically slow reaction rate of MTSET is probably due to the fact that the effective concentration of MTSET in the channel is much lower than the bulk concentration, a result of "sweeping" by the continuous influx of K^+ ions at a holding potential of −40 mV. Thus, the slow reaction rate is consistent with our interpretation that the reactive cysteines project into the aqueous vestibule. Indeed, if the reactive cysteines were on the surface of the channel protein and were exposed to the cytoplasm (but not the vestibule), one would expect that their reaction rate with MTSET approaches that of MTSET with free thiols in solution.

Two lysine-to-cysteine mutants, K64C and K219C, exhibited an increase of current after modification by MTSEA but were unaffected after modification by MTSET. Similar enhancement caused by modification by a MTS reagent has been shown for several putative pore-lining residues in membrane-spanning regions of *N*-methyl-D-aspartate (NMDA) receptor channels (28). How could covalent linkage of MTSEA to putative vestibule-lining cysteines in K64C and K219C channels increase the current, whereas linkage of MTSET has no effect? A clue may come from comparisons of the side-chain changes at these positions as a result of the covalent modifications. Cysteine has a side chain of -CH_2-SH; after covalent reaction with MTSEA, the side chain becomes -CH_2-S-S-CH_2-CH_2-NH_3^+. This structure is similar in length (albeit ≈2.6 Å longer) to the lysine side chain (-CH_2-CH_2-CH_2-CH_2-NH_3^+) and has the same -H_3^+ head group (≈3.6 Å in diameter). On the other hand, covalent modification by MTSET results in a side chain of -CH_2-S-S-CH_2-CH_2-N$(CH_3)_3^+$, which is ≈3.7 Å longer than the lysine side chain and has a trimethylammonium head group (≈5.8 Å in diameter) whose polarity, solvation,

and size are different from $-NH_3^+$. Thus, covalent modification of the cysteine mutant channels by MTSEA, but not MTSET, may convert them to behave similarly to the wild-type channels and hence result in an increase instead of a decrease of current. We should point out, however, that it remains possible that C64 and C219 do not face the vestibule and their modification by MTSEA causes an allosteric structural change that results in an increase of channel activity.

The interpretation that the amino-terminal segment adjacent to M1 contributes to form the intracellular vestibule of Kir channels is in line with work on voltage-gated K^+ channels, where the equivalent S4–S5 loop was found to interact with permeant and blocking ions as well as the inactivation particle (29, 30). The surprising aspect is the extent to which the amino-terminal segment is involved—15 of 33 residues possibly face the vestibule, including an amino acid (C54) as far as 30 residues away from M1. Positions corresponding to C54 have recently been shown to be reactive with sulfhydryl-modifying reagents in other Kir channels in a state-dependent manner (31, 32). For example, C49 in Kir1.1 channels can be modified by 5,5′-dithiobis(2-nitrobenzoic acid) only in the closed state (32). On the other hand, C42 in Kir6.2 channels can be modified by *p*-chloromercuriphenylsulfonate only in the open state (31). It is unclear what accounts for the discrepancy between these studies, though the use of different types of channels and modifying reagents may contribute. We did not examine the state dependence of modification, but because Kir2.1 channels have a high open probability of 0.9 (unpublished observations), we speculate that modification of C54 occurs in the open state.

The results in this study allow us to deduce several molecular features of the intracellular vestibule of Kir2.1 channels. First, the pattern of accessibility to MTSEA and MTSET (Figs. 2 and 3) indicates that the two vestibule-forming regions do not have a periodic secondary structure. Clusters of 4 or 5 reactive positions were found in both segments. Such a side-chain projection pattern is incompatible with an α-helical or β-sheet structure. Instead, it suggests that both regions adopt an extended loop structure. Second, the finding of a large number of putative pore-lining residues in the cytoplasmic amino and carboxyl domains suggests that they form a long intracellular vestibule extending from the membrane into the cytoplasm. Third, the intracellular vestibule is wide, with a diameter of at least 20 Å. This conclusion is primarily based on the finding that at position E224, the vestibule appears wide enough to simultaneously accommodate four qBBr moieties with overall dimensions of 12 Å × 10 Å × 6 Å (Fig. 5). We have previously shown that the inner pore formed by M2 can accommodate two or three but not four qBBr moieties (19). Thus, the intracellular vestibule formed by the cytoplasmic regions is most likely wider than the inner pore formed by the M2 segment.

We thank Dr. Steven Siegelbaum for careful reading of and insightful comments on a previous version of the manuscript. This work was supported by an Alfred P. Sloan Research Fellowship and by National Institutes of Health Research Grant HL58552.

1. Hille, B. (1992) *Ionic Channels of Excitable Membranes* (Sinauer, Sunderland, MA), pp. 127–130.
2. Hagiwara, S., Miyazaki, S. & Rosenthal, N. P. (1976) *J. Gen. Physiol.* **67,** 621–638.
3. Matsuda, H., Saigusa, A. & Irisawa, H. (1987) *Nature (London)* **325,** 156–158.
4. Vandenberg, C. A. (1987) *Proc. Natl. Acad. Sci. USA* **84,** 2560–2564.
5. Matsuda, H. (1988) *J. Physiol. (London)* **397,** 237–258.
6. Ishihara, K., Mitsuiye, T., Noma, A. & Takano, M. (1989) *J. Physiol. (London)* **419,** 297–320.
7. Lu, Z. & MacKinnon, R. (1994) *Nature (London)* **371,** 243–246.
8. Nichols, C. G., Ho, K. & Hebert, S. (1994) *J. Physiol.* **476,** 399–409.
9. Stanfield, P. R., Davies, N. W., Shelton, P. A., Sutcliffe, M. J., Khan, I. A., Brammar, W. J. & Conley, E. C. J. (1994) *J. Physiol. (London)* **478,** 1–6.
10. Taglialatela, M., Wible, B. A., Caporaso, R. & Brown, A. M. (1994) *Science* **264,** 844–847.
11. Ficker, E., Taglialatela, M., Wible, B. A., Henley, C. M. & Brown, A. M. (1994) *Science* **266,** 1068–1072.
12. Lopatin, A. N., Makhina, E. N. & Nichols, C. G. (1994) *Nature (London)* **372,** 366–369.
13. Fakler, B., Brandle, U., Glowatzki, E., Weidemann, S., Zenner, H.-P. & Ruppersberg, J. P. (1995) *Cell* **80,** 149–154.
14. Ho, K., Nichols, C. G., Lederer, W. J., Lytton, J., Vassilev, P. M., Kanazirska, M. V. & Hebert, S. C. (1993) *Nature (London)* **362,** 31–38.
15. Kubo, Y., Baldwin, T. J., Jan, Y. N. & Jan, L. Y. (1993) *Nature (London)* **362,** 127–133.
16. Doyle, D. A., Cabral, J. M., Pfuetzner, R. A., Kuo, A., Gulbis, J. M., Cohen, S. L., Chait, B. T. & MacKinnon, R. (1998) *Science* **280,** 69–77.
17. Akabas, M. H., Stauffer, D. A., Xu, M. & Karlin, A. (1992) *Science* **258,** 307–310.
18. Karlin, A. & Akabas, M. H. (1998) *Methods Enzymol.* **293,** 123–145.
19. Lu, T., Nguyen, B., Zhang, X. M. & Yang, J. (1999) *Neuron* **22,** 571–580.
20. Taglialatela, M., Ficker, E., Wible, B. A. & Brown, A. M. (1995) *EMBO J.* **14,** 5532–5541.
21. Yang, J., Jan, Y. N. & Jan, L. Y. (1995) *Neuron* **14,** 1047–1054.
22. Fakler, B., Schultz, J., Yang, J., Schulte, U., Brandel, U., Zenner, H. P., Jan, L. Y. & Ruppersberg, J. P. (1996) *EMBO J.* **15,** 4093–4099.
23. Liman, E. R., Tytgat, J. & Hess, P. (1992) *Neuron* **9,** 861–871.
24. Yang, J., Jan, Y. N. & Jan, L. Y. (1995) *Neuron* **15,** 1441–1447.
25. Yang, J., Jan, Y. N. & Jan, L. Y. (1997) *Proc. Natl. Acad. Sci. USA* **94,** 1568–1572.
26. Stauffer, D. A. & Karlin, A. (1994) *Biochemistry* **33,** 6840–6849.
27. Kosower, N. S., Kosower, E. M., Newton, G. L. & Ranney, H. M. (1979) *Proc. Natl. Acad. Sci. USA* **76,** 3382–3386.
28. Beck, C., Wollmuth, L. P., Seeburg, P. H., Sakmann, B. & Kuner, T. (1999) *Neuron* **22,** 559–570.
29. Isacoff, E. Y., Jan, Y. N. & Jan, L. Y. (1991) *Nature (London)* **353,** 86–90.
30. Slesinger, P. A., Jan, Y. N. & Jan, L. Y. (1993) *Neuron* **11,** 739–749.
31. Trapp, S., Tucker, S. J. & Ashcroft, F. M. (1998) *J. Gen. Physiol.* **112,** 325–332.
32. Schulte, U., Hahn, H., Wiesinger, H., Ruppersberg, J. P. & Fakler, B. (1998) *J. Biol. Chem.* **273,** 34575–34579.